Excitation of Nonradiating Anapoles in Dielectric Nanospheres

John A. Parker,[2,3] Hiroshi Sugimoto,[4] Brighton Coe,[1] Daniel Eggena,[1] Minoru Fujii,[4] Norbert F. Scherer,[2,5] Stephen K. Gray,[6] and Uttam Manna[1,*]

[1]*Department of Physics, Illinois State University, Normal, Illinois 61709, USA*
[2]*The James Franck Institute, University of Chicago, Chicago, Illinois 60637, USA*
[3]*Department of Physics, University of Chicago, Chicago, Illinois 60637, USA*
[4]*Department of Electrical and Electronic Engineering, Graduate School of Engineering, Kobe University, Rokkodai, Nada, Kobe 657-8501, Japan*
[5]*Department of Chemistry, University of Chicago, Chicago, Illinois 60637, USA*
[6]*Center for Nanoscale Materials, Argonne National Laboratory, Lemont, Illinois 60439, USA*

(Received 14 August 2019; accepted 27 January 2020; published 6 March 2020)

Although the study of nonradiating anapoles has long been part of fundamental physics, the dynamic anapole at optical frequencies was only recently experimentally demonstrated in a specialized silicon nanodisk structure. We report excitation of the electrodynamic anapole state in *isotropic* silicon nanospheres using radially polarized beam illumination. The superposition of equal and out-of-phase amplitudes of the Cartesian electric and toroidal dipoles produces a pronounced dip in the scattering spectra with the scattering intensity almost reaching zero—a signature of anapole excitation. The total scattering intensity associated with the anapole excitation is found to be more than 10 times weaker for illumination with radially vs linearly polarized beams. Our approach provides a simple, straightforward alternative path to realizing nonradiating anapole states at the optical frequencies.

DOI: 10.1103/PhysRevLett.124.097402

Nonradiating sources are special configurations of charge-current distributions that do not radiate in the far field [1,2]. Historically, nonradiating sources attracted a lot of attention in the field of quantum mechanics in the context of radiationless motion [3], extended electron models [4], as well as providing possible scenarios for observing a dynamic Aharonov-Bohm effect [5]. Recently, there is a growing interest in nonradiating sources in nanophotonics and quantum optics because of their ability to highly confine electromagnetic fields in subwavelength structures [6–15]; of particular interest are bound states in the continuum [6–8] and *anapole* states [9–13].

Bound states in the continuum, which are embedded eigenstates of an open cavity, are characterized by resonant frequencies lying in the continuum spectrum of radiating modes within the structures [6–8]. On the contrary, anapoles are not inherent states of a resonant structure but dynamic excitations, which depend strongly on external parameters such as the properties of the incident beam or the excitation geometry [9–13,16], as typically done in the context of cloaking devices [17]. More specifically, for time-varying oscillating charge-current distributions, electrodynamic anapoles are related to the so-called electrodynamic *toroidal* dipoles corresponding to current flows on the surface of a torus [18]. The superposition of the scattered fields of conventional and toroidal dipoles that have the same amplitude but are out of phase can result in the total cancellation of far-field scattering amplitude. This cancellation of far-field scattering amplitude is termed a nonradiating electrodynamic anapole [9–13]. It has been predicted that efficient excitation of the nonradiating anapole states can give rise to enhanced nonlinear effects [19–21], nanolasers [22], ideal magnetic scattering [23], broadband absorption [24], metamaterials and metasurfaces [25], as well as extremely high Q factors ($\sim 10^6$) and near-field enhancements [26,27].

Despite the concept of a toroidal dipole mode existing in the literature since the 1980s [28,29], the interfering state of toroidal and conventional dipoles or simply the anapole, was experimentally demonstrated in composite structures in the microwave regime only in 2013 [10], and within specially designed individual dielectric nanodisks at optical frequencies only in 2015 [9]. Detection of anapoles requires the design of specialized structures, such as nanodisks [9], radially anisotropic nanospheres [30], and core-shell nanostructures [31,32] so that the dominant contribution of scattering comes from the electric and toroidal dipole mode with all other modes strongly suppressed. As a result, it is not possible to detect the anapole states in isotropic spheres under plane wave illumination [9,11,13,33], because both electric multipoles and (adjacent) *magnetic* multipoles are excited from spherically symmetric nanoobjects, preventing a perfect cancelation of the far-field scattering.

However, fabrication of these highly specialized structures requires complex nanofabrication, which makes experimental observation of anapoles in these proposed specialized

structures not feasible at this time. To this end, it would be desirable to be able to excite anapoles in simple nanostructures, such as a nanosphere without relying on the fabrication of complex nanostructures. Recently, Urbach and co-workers [33] theoretically proposed that one could possibly excite nonradiating anapoles within high-index isotropic nanospheres using a tightly focused radially polarized cylindrical vector beam (CVB).

In this Letter, we report experimental excitation of the electrodynamic anapole state within isotropic nanospheres using a tightly focused radially polarized CVB. Specifically, we show that the radially polarized CVBs [33–37] allow selective excitation of electric multipoles, and hence the anapole state within silicon (Si) nanospheres. Radially and azimuthally polarized CVBs have been previously used to selectively excite and enhance multipolar resonances in a number of material systems [38–40]. Our experimental results show that for certain wavelengths ($\lambda \sim 500$ nm for nanosphere diameter, $d \sim 160$ nm; and $\lambda \sim 520$ nm for $d \sim 180$ nm), the (total) scattering intensity shows pronounced dip with the scattering intensity almost reaching zero, and the scattering intensity is more than 10 times weaker for illumination with radially vs linearly polarized beams. The results of electrodynamic simulations show that the anapole conditions are satisfied at wavelengths at which the scattering minima appear in the experimental spectra, and the internal energy is approximately 6 times greater for illumination with radially vs linearly polarized beams.

Our results demonstrate that we are capable of exciting electrodynamic anapole states in high-index (Si) nanoparticles having spherical geometry. Since the particular polarization property of the illumination is responsible for the anapole excitation by suppressing unwanted magnetic modes in the nanosphere, our approach provides a simple, straightforward alternative path to realize the aforementioned intriguing possibilities [19–27], such as extremely high Q factors ($\sim 10^6$) and near-field enhancements [26,27] without relying on the design of specialized structures.

Theoretical considerations.—The Cartesian electric dipole moment at frequency ω is given by [9]

$$\boldsymbol{P}(\omega) = \frac{i}{\omega}\int_V \boldsymbol{J}(\omega)d\boldsymbol{r}, \tag{1}$$

with

$$\boldsymbol{J}(\omega) = -i\omega\varepsilon_0[\varepsilon_r - 1]\boldsymbol{E}(\omega), \tag{2}$$

being the induced current density produced by the electric field, $\boldsymbol{E}$, ε_r is the relative permittivity of Si, and the integral in Eq. (1) is over the volume of the nanosphere, V. In our Fourier representation, we omit the $\exp(-i\omega t)$ time dependence of the fields. In addition to the excitation of $\boldsymbol{P}$, the incident field also excites a current density in the form of a toroidal dipole moment given by

$$\boldsymbol{T}(\omega) = \frac{1}{10c}\int_V \{[\boldsymbol{r}\cdot\boldsymbol{J}(\omega)]\boldsymbol{r} - 2r^2\boldsymbol{J}(\omega)\}d\boldsymbol{r}. \tag{3}$$

Therefore, the total dipolar contribution to the far-field radiation is

$$\boldsymbol{E}_{\text{scat}}(\boldsymbol{r},\omega) \sim \frac{k^2}{4\pi\varepsilon_0 r}[\hat{\boldsymbol{r}}\times\boldsymbol{P}(\omega)\times\hat{\boldsymbol{r}} + ik\hat{\boldsymbol{r}}\times\boldsymbol{T}(\omega)\times\hat{\boldsymbol{r}}], \tag{4}$$

where $\hat{\boldsymbol{r}}$ is the normalized vector of the observation direction. The scattered far-field radiation, $\boldsymbol{E}_{\text{scat}}$, will vanish if

$$\boldsymbol{P}(\omega) = -ik\boldsymbol{T}(\omega). \tag{5}$$

That is, the contributions of the Cartesian electric and toroidal dipoles to the scattered field are equal and out of phase—this is the condition for anapole excitation [9].

Observation of a nonradiating anapole state requires proper electric and toroidal dipole excitation, and the suppression of other multipole modes which can contribute to the total scattered power. It was proposed that one could possibly satisfy these requirements by selective excitation of the electric modes in dielectric nanospheres having a refractive index, $n = 3.5$ and $d = 200$ nm using radially polarized beams [33]. Having $n \sim 3.5$–4.0 [41], Si nanospheres with $d \sim 150$–200 nm would be ideal candidates to validate the excitation of electrodynamic anapoles using radially polarized beams experimentally. A schematic of this idea is shown in Fig. 1(a). The selective excitation of electric modes by a focused radially polarized beam can be explained by the multipole expansion of the scattered field [33,42,43]:

$$\boldsymbol{E}_{\text{scat}}(\boldsymbol{r},\omega) = \sum_{l=1}^{\infty}\sum_{m=-l}^{l}[p^0_{Eml}(\omega)\boldsymbol{N}^0_{ml}(\boldsymbol{r},\omega) + p^0_{Mml}(\omega)\boldsymbol{M}^0_{ml}(\boldsymbol{r},\omega)], \tag{6}$$

where $\boldsymbol{N}^0_{ml}(\boldsymbol{r},\omega)$ and $\boldsymbol{M}^0_{ml}(\boldsymbol{r},\omega)$ are the vector spherical harmonics associated with the electric and magnetic modes, and $p^0_{Eml}(\omega)$ and $p^0_{Mml}(\omega)$ are the strengths of the electric and magnetic components, respectively. For an on-axis radially polarized beam, $p^0_{Mml}(\omega) = 0$; i.e., all the magnetic multipole components are zero.

The distributions of the local fields calculated for a Si nanosphere with $d = 160$ nm for radially polarized beam excitation using a generalized Mie theory (GMT) [44,45] are shown in Fig. 1(b). The GMT simulations reveal that the toroidal current is produced by currents flowing on the surface of the Si nanosphere along the z direction, i.e., the beam propagation direction. Hence, destructive interference of the z component of the fields scattering from a Cartesian dipole moment and toroidal dipole moment of a Si nanosphere for a radially polarized beam can completely cancel the scattering amplitude in the far field.

Experimental and simulation considerations.—The Si nanospheres were synthesized colloidally from Si-rich borophosphosilicate glass as reported previously [46]. A brief description of synthesis and the transmission electron

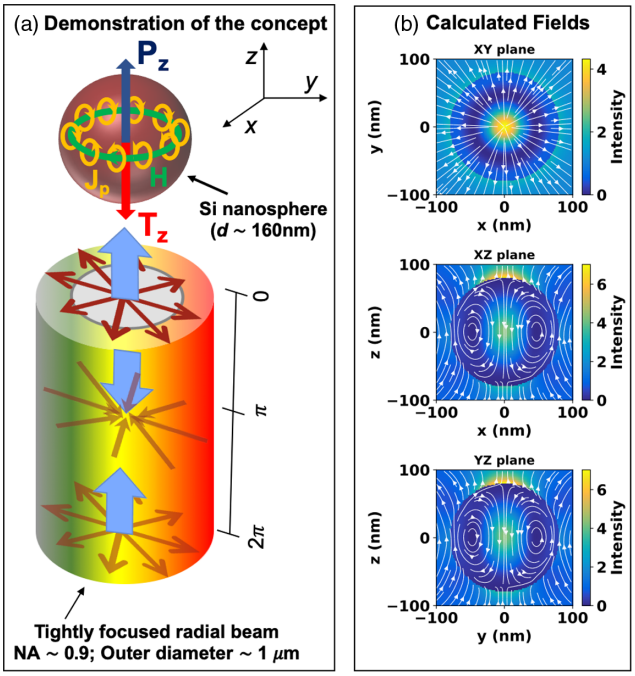

FIG. 1. Demonstration of the anapole excitation and simulated electric field distributions. (a) Schematic diagram showing excitation of a Si nanosphere ($d \sim 160$ nm) for radially polarized beam excitation. In addition to the z component of the electric resonances ($\mathbf{P}_z$), the radially polarized beam is expected to generate a z component of the toroidal response ($\mathbf{T}_z$) produced by the circulating magnetic field ($\mathbf{H}$) associated with the poloidal currents ($\mathbf{J}_p$) flowing in the bulk. (b) Streamlines of the total electric field for radially polarized beam illumination as calculated using generalized Mie theory show that the toroidal current [given by Eq. (3)] is indeed produced within the volume of the nanosphere.

microscope image showing almost perfect spherical shape of the nanoparticles is provided in Sec. I in the Supplemental Material (SM) [47]. The solutions of Si nanospheres were drop cast and dried on a glass substrate before measurement. The scattering spectra of single Si nanospheres were measured using a broadband vector beam scattering spectroscopy that we developed recently [39,51]. Briefly, the output of a spatially coherent broadband continuum was sent through a liquid crystal polarization converter, which was then coupled to an inverted optical microscope equipped with a 40× air objective with numerical aperture, NA ≤ 0.9. The back-reflected scattering spectra of single Si nanospheres were recorded by a CCD connected to an imaging spectrometer coupled to the side port of the microscope via a homebuilt achromatic $4f$ relay system. The details of the experimental setup are described in Sec. II in the SM. Figure 2 shows the experimentally measured [Figs. 2(a) and 2(c)] and corresponding simulated [Figs. 2(b) and 2(d)] scattering spectra of single Si nanospheres with $d \sim 160$ nm [Figs. 2(a) and 2(b)], and $d \sim 180$ nm [Figs. 2(c) and 2(d)] for linearly, radially, and azimuthally polarized beam illuminations. The diameters of the nanospheres were found by taking correlated SEM images as shown in the inset of Figs. 2(a) and 2(c). The details on how correlated optical and SEM measurements are performed at the single nanoparticle level are described in Sec. III in the SM. The electrodynamic simulations were performed by GMT in the presence of a glass-air interface, as described elsewhere [44,45]. The simulation details are described in Sec. IV in the SM.

Single Si nanoparticle scattering spectra.—The experimental and simulated scattering spectra (Fig. 2) show several peaks within the measurement window ($\lambda =$ 420–750 nm) for linearly polarized beam illumination. On the other hand, only some of the peaks are selectively excited for radially and azimuthally polarized beam illuminations. Interestingly, the results also show that the scattering minima are deepest for radially polarized beam excitation at around 500 nm for $d = 160$ nm [Figs. 2(a) and 2(b)], and at around 520 nm for $d = 180$ nm [Figs. 2(c) and 2(d)] Si nanospheres (the regions of interest are shown in the insets). The calculated peak positions and relative scattering of the various illuminations agree quite well with the experiments with the exception of relative intensities of the electric and magnetic dipole modes. This is because the experimental scattering spectra were measured in the backward direction for a limited angular range determined by the numerical aperture (NA) of the objective lens, whereas the simulated scattering spectra were calculated over all scattering angles. See Sec. V of the SM for a detailed discussion on the dependence of the calculated scattering spectra on the simulation geometry.

Multipolar decomposition of the scattering spectra.—We performed a multipolar decomposition of the scattered fields [39,51,52] to understand the nature of the peaks appearing in the Si nanosphere scattering spectra for various beam illuminations. The results of the multipolar decomposition of the scattered fields are shown in Fig. 3 for $d = 160$ nm Si nanoparticles for linearly, radially, and azimuthally polarized beam illuminations. The results of the multipolar decomposition of the scattered fields for $d =$ 180 nm is shown in Fig. S8 in the SM. The results show that (i) both the electric and magnetic multipoles (dipolar and quadrupolar) are excited for linearly polarized beam illumination; (ii) only the electric multipoles are excited (dipolar and quadrupolar) for radially polarized beam illumination; (iii) only the magnetic multipoles are excited (dipolar and quadrupolar) for azimuthally polarized beam illumination; and (iv) the toroidal dipoles are also excited for linearly and radially polarized beam illuminations (discussed in more detail below). Since the radially polarized beam only excites the electric multipoles and suppresses all the magnetic modes in the nanospheres, our scheme is essentially analogous to illumination of nanodisks with linearly polarized beams [9] which satisfy the anapole excitation condition of Eq. (5). Is the anapole excitation condition [Eq. (5)] satisfied in the Si nanosphere

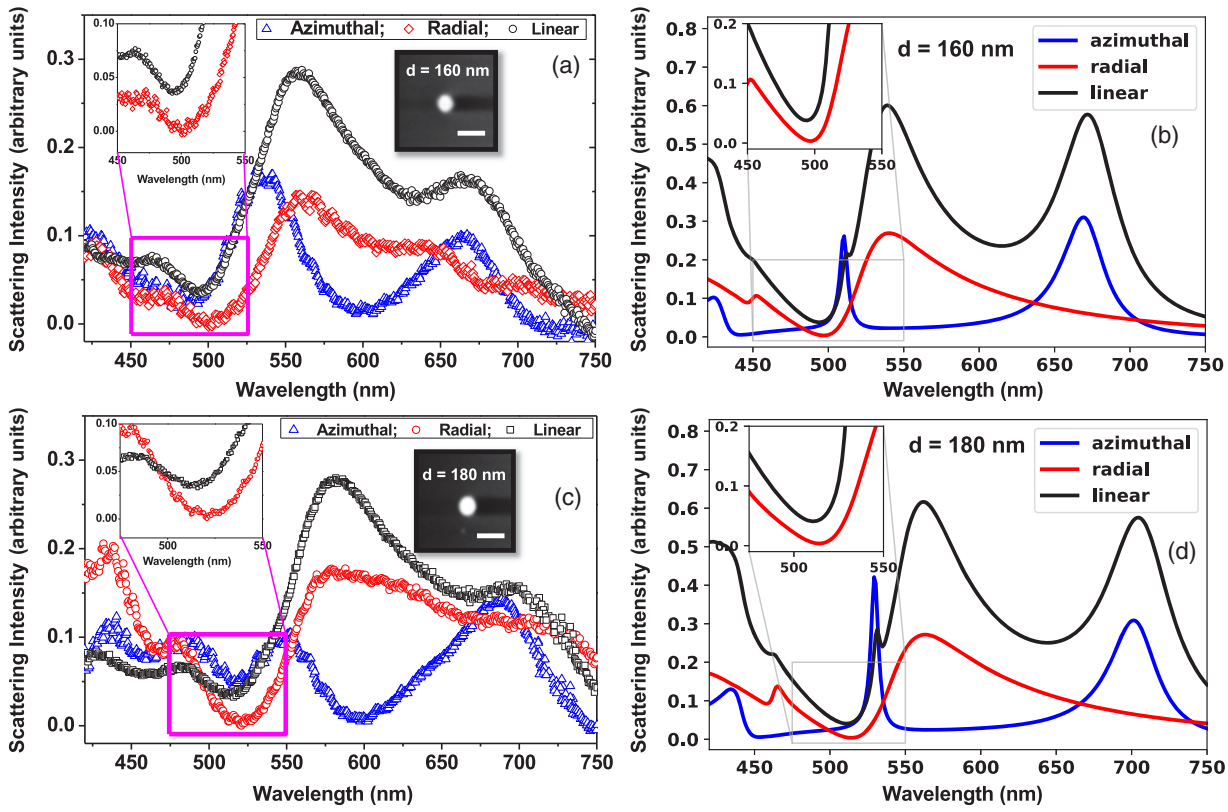

FIG. 2. Scattering spectra of single Si nanospheres under linear and vector beam illumination. The experimental (a),(c) and simulated (b),(d) scattering spectra of single Si nanospheres with diameter 160 (a),(b) and 180 nm (c),(d), respectively, for linearly, radially, and azimuthally polarized beam illuminations. The right insets of (a) and (c) show the SEM images of the exact same nanospheres whose scattering spectra are shown. The white scale bars on the SEM images are 500 nm. The results show that the scattering minima are deepest for radial beam excitation at around 500 nm (the regions of interest is shown in the insets) for $d = 160$ nm (a),(b), and at around 520 nm for $d = 180$ nm (c),(d). The simulated spectra were calculated using generalized Mie theory over all the scattering angles, whereas the experimental spectra were measured in the backward direction for the angular range determined by the numerical aperture of the microscope objective.

for radially polarized beam illumination? We investigate this possibility next.

Criterion for anapole excitation in spherical nanoparticles.—In addition to the selective excitation of the electric multipoles, the experimentally measured scattering spectra are also accompanied by a deeper minimum with the scattering intensity almost reaching zero for radially polarized beam illumination (red curve) at $\lambda \sim 500$ nm for

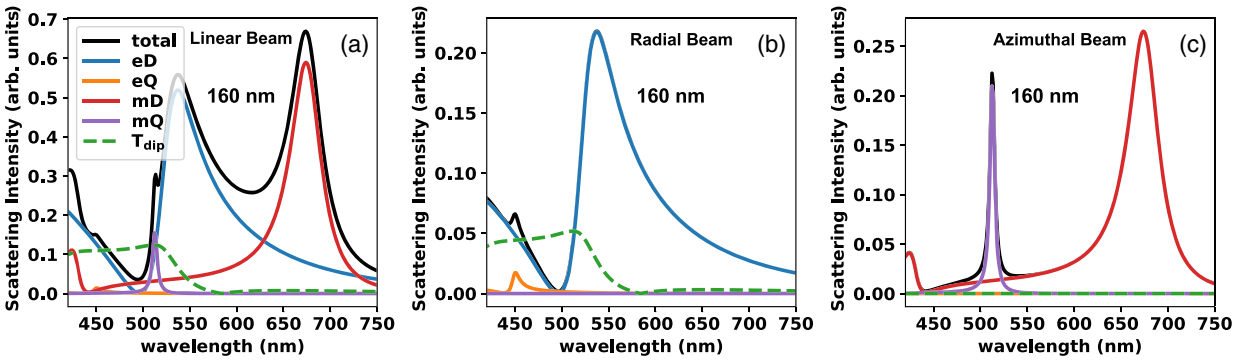

FIG. 3. Multipolar decomposition of the scattering spectra. The calculated scattering spectra of single Si nanospheres with diameter $d = 160$ nm for linearly (a), radially (b), and azimuthally (c) polarized beam illuminations. The multipolar decomposition shows that both electric and magnetic modes are excited for linearly polarized beam; whereas only electric (magnetic) modes are excited for radially (azimuthally) polarized beam illumination. The toroidal dipoles are also excited for linearly and radially polarized beam illuminations.

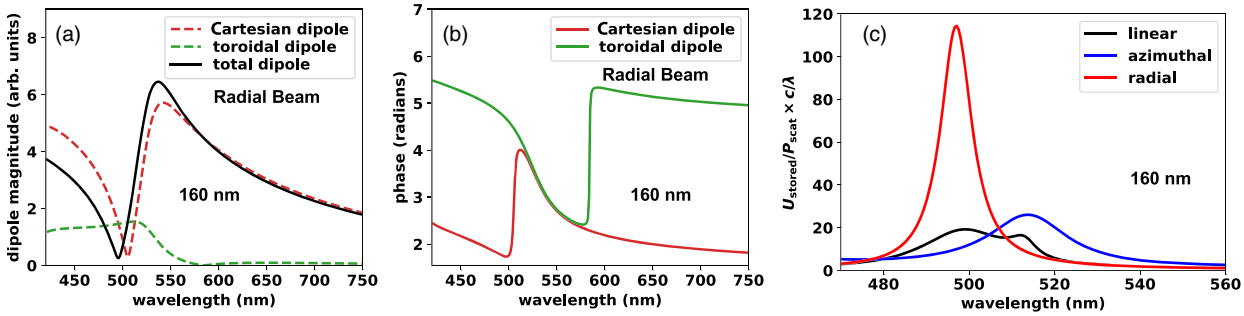

FIG. 4. The amplitude (a) and phase (b) of the Cartesian electric and toroidal dipoles under radially polarized beam illumination for $d = 160$ nm. The results show that the amplitudes of the Cartesian electric and toroidal dipoles are equal and out of phase at $\lambda \sim 500$ nm for $d = 160$ nm resulting in excitation of the anapole. (c) shows the fraction of the localized vs radiated energy calculated for linear, radial, and azimuthal beam illuminations for $d = 160$ nm. The stored energy is ~6 times greater for radial vs linear beam illumination.

$d \sim 160$ nm [Figs. 2(a) and 2(c)], and at $\lambda \sim 520$ nm for $d \sim 180$ nm [Figs. 2(b) and 2(d)] diameter nanospheres as shown in Fig. 2. Moreover, the results of the multipolar decomposition (Fig. 3) show that there is a finite contribution from the toroidal dipole excitation (green dashed curves) due to the excitation of the z component of the toroidal moment [Fig. 1(b)].

To determine if the scattering minima arise from the excitation of an anapole state in the Si nanospheres, we calculated the amplitude and phase of the Cartesian electric and toroidal dipoles for $d = 160$, and 180 nm for radially polarized beam illumination. The results show that the amplitudes of the Cartesian electric and toroidal dipoles are indeed equal and out of phase, that is, Eq. (5) is satisfied at $\lambda \sim 500$ nm for $d \sim 160$ nm [as shown in Figs. 4(a) and 4(b)] and at $\lambda \sim 520$ nm for $d \sim 180$ nm [as shown in Figs. S9(a) and S9(b) in the SM]. The concurrent appearance of a scattering minimum along with equal but out of phase amplitudes of the Cartesian electric and toroidal dipoles at the same wavelength confirms the excitation of the electrodynamic anapole state in the Si nanospheres for radially polarized beam illumination. Our results agree with calculated results previously reported by Urbach and co-workers [33].

The total scattering intensity at the anapole condition is found to be more than 10 times weaker for the radially polarized beam illumination compared to linearly polarized beam illumination [Figs. 2(a) and 2(c)] as found both in the calculations and experiments. For details on estimation of error and reduction in the scattering intensities for radially vs linearly polarized beams, see Sec. VIII of the SM. We have also calculated the fraction of the localized vs radiated energy for linear, radial, and azimuthal beam illuminations as shown in Fig. 4(c) for $d = 160$ nm. The results for $d = 180$ nm are shown in Fig. S9(c) in the SM. The results show that the stored energy normalized to the scattered power ($U_{\text{stored}}/P_{\text{scat}} \times c/\lambda$, in units of cycles of radiation) for radial beam illumination is approximately 6 times greater compared to linear beam illumination. Note that the scattering spectra for the azimuthal beam illumination also show a pronounced dip (Fig. 2) at approximately the same wavelengths at which the anapole condition is satisfied. However, the cause of this pronounced dip is not due to an interference of two modes, rather due to the selective excitation of an effectively nonexistent magnetic dipole. Hence, for azimuthal beam illumination there is no confinement of the electromagnetic energy within the volume of the nanospheres.

In conclusion, the discovery of the electrodynamic anapole state is a major step towards stronger confinement of electromagnetic fields in subwavelength dielectric nanostructures having much weaker or almost negligible losses. However, the excitation of the anapole state requires fabrication of highly specialized structures, and has only been previously demonstrated in a highly specialized structure in the form of a Si nanodisk at optical frequencies. Here, we report experimental demonstration of electrodynamic anapole in Si nanospheres using radially polarized beam illumination with the scattering intensity almost reaching zero at the anapole condition. Hence, our approach provides a simple, straightforward alternative path to excite anapole states without relying on the design of specialized structures. This opens up a new route to realizing predicted enhanced nonlinear effects, nanolasers, ideal magnetic scattering, as well as extremely high Q factors ($\sim 10^6$) associated with anapole states. Note that for radially polarized beam illumination, the electric quadrupole mode still contributes very weakly to the total scattering spectra [Fig. 2(d)], which could be suppressed by illumination of the nanosphere with a counterpropagating radially polarized beam leading to excitation of an "ideal" anapole state, similar to the proposal made by Urbach and co-workers [33]; we are currently working on this possibility.

This material is based upon work supported by the National Science Foundation (NSF) under Grant No. ECCS-1809410. H. S. and M. F. acknowledge KAKENHI Grants No. 18K14092 and No. 18KK0141 from Japan Society for the Promotion of Science. J. A. P. and N. F. S. acknowledge support from the Vannevar Bush Faculty

Fellowship program sponsored by the Basic Research Office of the Assistant Secretary of Defense for Research and Engineering and funded by the Office of Naval Research through Grant No. N00014-16-1-2502. We thank the W. M. Keck Foundation for partial support. This work was performed, in part, at the Center for Nanoscale Materials, a U.S. Department of Energy Office of Science User Facility, and supported by the U.S. Department of Energy, Office of Science, under Contract No. DE-AC02-06CH11357. We also acknowledge the University of Chicago Research Computing Center for providing the computational resources needed for this work.

*umanna@ilstu.edu

[1] K. Kim and E. Wolf, Opt. Commun. **59**, 1 (1986).
[2] A. J. Devaney and E. Wolf, Phys. Rev. D **8**, 1044 (1973).
[3] D. Bohm and M. Weinstein, Phys. Rev. **74**, 1789 (1948).
[4] P. Pearle, Found. Phys. **8**, 879 (1978).
[5] N. A. Nemkov, A. A. Basharin, and V. A. Fedotov, Phys. Rev. B **95**, 165134 (2017).
[6] C. W. Hsu, B. Zhen, A. D. Stone, J. D. Joannopoulos, and M. Soljacic, Nat. Rev. Mater. **1**, 16048 (2016).
[7] C. W. Hsu, B. Zhen, J. Lee, S. L. Chua, S. G. Johnson, J. D. Joannopoulos, and M. Soljacic, Nature (London) **499**, 188 (2013).
[8] F. Monticone and A. Alu, Phys. Rev. Lett. **112**, 213903 (2014).
[9] A. E. Miroshnichenko, A. B. Evlyukhin, Y. F. Yu, R. M. Bakker, A. Chipouline, A. I. Kuznetsov, B. Luk'yanchuk, B. N. Chichkov, and Y. S. Kivshar, Nat. Commun. **6**, 8069 (2015).
[10] V. A. Fedotov, A. V. Rogacheva, V. Savinov, D. P. Tsai, and N. I. Zheludev, Sci. Rep. **3**, 2967 (2013).
[11] K. V. Baryshnikova, D. A. Smirnova, B. S. Luk'yanchuk, and Y. S. Kivshar, Adv. Opt. Mater. **7**, 1801350 (2019).
[12] V. Savinov, N. Papasimakis, D. P. Tsai, and N. I. Zheludev, Commun. Phys. **2**, 69 (2019).
[13] K. Koshelev, G. Favraud, A. Bogdanov, Y. Kivshar, and A. Fratalocchi, Nanophotonics **8**, 725 (2019).
[14] M. Kerker, J. Opt. Soc. Am. **65**, 376 (1975).
[15] R. Fleury, F. Monticone, and A. Alu, Phys. Rev. Applied **4**, 037001 (2015).
[16] F. Monticone, D. Sounas, A. Krasnok, and A. Alù, https://arxiv.org/abs/1908.00956 (2019).
[17] A. K. Ospanova, G. Labate, L. Matekovits, and A. A. Basharin, Sci. Rep. **8**, 12514 (2018).
[18] N. Papasimakis, V. A. Fedotov, V. Savinov, T. A. Raybould, and N. I. Zheludev, Nat. Mater. **15**, 263 (2016).
[19] W.-C. Zhai, T.-Z. Qiao, D.-J. Cai, W.-J. Wang, J.-D. Chen, Z.-H. Chen, and S.-D. Liu, Opt. Express **24**, 27858 (2016).
[20] G. Grinblat, Y. Li, M. P. Nielsen, R. F. Oulton, and S. A. Maier, ACS Nano **11**, 953 (2017).
[21] G. Grinblat, Y. Li, M. P. Nielsen, R. F. Oulton, and S. A. Maier, Nano Lett. **16**, 4635 (2016).
[22] J. S. T. Gongora, A. E. Miroshnichenko, Y. S. Kivshar, and A. Fratalocchi, Nat. Commun. **8**, 15535 (2017).
[23] T. H. Feng, Y. Xu, W. Zhang, and A. E. Miroshnichenko, Phys. Rev. Lett. **118**, 173901 (2017).
[24] R. Wang and L. Dal Negro, Opt. Express **24**, 19048 (2016).
[25] A. K. Ospanova, I. V. Stenishchev, and A. A. Basharin, Laser Photonics Rev. **12**, 1800005 (2018).
[26] S. D. Liu, Z. X. Wang, W. J. Wang, J. D. Chen, and Z. H. Chen, Opt. Express **25**, 22375 (2017).
[27] A. A. Basharin, V. Chuguevsky, N. Volsky, M. Kafesaki, and E. N. Economou, Phys. Rev. B **95**, 035104 (2017).
[28] A. Costescu and E. E. Radescu, Phys. Rev. D **35**, 3496 (1987).
[29] G. N. Afanasiev and V. M. Dubovik, Phys. Part. Nucl. **29**, 366 (1998).
[30] W. Liu, B. Lei, J. Shi, H. Hu, and A. E. Miroshnichenko, J. Nanomater. **2015**, 672957 (2015).
[31] W. Liu, J. F. Zhang, and A. E. Miroshnichenko, Laser Photonics Rev. **9**, 564 (2015).
[32] W. Liu, J. F. Zhang, B. Lei, H. J. Hu, and A. E. Miroshnichenko, Opt. Lett. **40**, 2293 (2015).
[33] L. Wei, Z. Xi, N. Bhattacharya, and H. P. Urbach, Optica **3**, 799 (2016).
[34] D. G. Hall, Opt. Lett. **21**, 9 (1996).
[35] K. S. Youngworth and T. G. Brown, Opt. Express **7**, 77 (2000).
[36] Q. Zhan, Adv. Opt. Photonics **1**, 1 (2009).
[37] L. Novotny and B. Hecht, *Principles of Nano-Optics* (Cambridge University Press, Cambridge, England, 2006).
[38] M. Kasperczyk, S. Person, D. Ananias, L. D. Carlos, and L. Novotny, Phys. Rev. Lett. **114**, 163903 (2015).
[39] U. Manna, J.-H. Lee, T.-S. Deng, J. Parker, S. Shepherd, Y. Weizmann, and N. F. Scherer, Nano Lett. **17**, 7196 (2017).
[40] P. Wozniak, P. Banzer, and G. Leuchs, Laser Photonics Rev. **9**, 231 (2015).
[41] G. Vuye, S. Fisson, V. N. Van, Y. Wang, J. Rivory, and F. Abeles, Thin Solid Films **233**, 166 (1993).
[42] H. X. Thanh, X. Chen, and C. J. R. Sheppard, Phys. Rev. A **86**, 033817 (2012).
[43] T. A. Nieminen, H. Rubinsztein-Dunlop, and N. R. Heckenberg, J. Quant. Spectrosc. Radiat. Transfer **79–80**, 1005 (2003).
[44] J. A. Lock and G. Gouesbet, J. Quant. Spectrosc. Radiat. Transfer **110**, 800 (2009).
[45] D. W. Mackowski, J. Quant. Spectrosc. Radiat. Transfer **109**, 770 (2008).
[46] H. Sugimoto and M. Fujii, Adv. Opt. Mater. **5**, 1700332 (2017).
[47] See Supplemental Material at http://link.aps.org/supplemental/10.1103/PhysRevLett.124.097402 for details of synthesis of Si nanospheres, experimental setup, correlated SEM and Optical microscopy, and dependence of calculated scattering spectra on simulation geometry, which includes Refs. [48–50].
[48] M. Stalder and M. Schadt, Opt. Lett. **21**, 1948 (1996).
[49] G. Gouesbet and G. Gréhan, *Generalized Lorenz-Mie Theories* (Springer, Berlin, 2011), Vol. 31.
[50] H. Thanh Xuan, X. Chen, and C. J. R. Sheppard, J. Opt. Soc. Am. A **29**, 32 (2012).
[51] T. S. Deng, J. Parker, Y. Yifat, N. Shepherd, and N. F. Scherer, J. Phys. Chem. C **122**, 27662 (2018).
[52] J. A. Parker, S. K. Gray, and N. F. Scherer, arXiv:1711.06833v2.